

Article

γ -Ray Log Tool for Detecting the Presence of Low-Permeability Lenses in High-Resolution Modelling of Contaminated Sites

Stefania Franchini ¹, Francesco Maria De Filippi ^{1,*} , Maurizio Barbieri ^{2,*}  and Giuseppe Sappa ¹ 

¹ Department of Civil, Environmental and Construction Engineering (DICEA), Sapienza University of Rome, 00185 Rome, Italy; stefania.franchini@uniroma1.it (S.F.); giuseppe.sappa@uniroma1.it (G.S.)

² Department of Chemical Engineering Materials Environment (DICMA), Sapienza University of Rome, 00185 Rome, Italy

* Correspondence: francescomaria.defilippi@uniroma1.it (F.M.D.F.); maurizio.barbieri@uniroma1.it (M.B.)

Abstract: In contaminated sites, remediation measures mostly depend on previous high-resolution site characterization (HRSC) results. In the case of industrial sites, where there is a high pollution risk for groundwater, many hydrogeological models are often achieved using stratigraphy results of geological drilling after the monitoring network design. This approach is only sometimes possible when contaminant back diffusion from small low-permeability lenses and layers occurs within a high-permeability aquifer. This framework needs a significant resolution that can be obtained by coupling preliminary stratigraphic data with specific in situ activities. Results from these additional investigations may help to locate low-permeability layers and, consequently, to identify the most vulnerable areas towards which groundwater management must be deepened. The use of gamma rays in combination with the analysis of the pluviometric and hydrometric data and together with the time series of the concentrations of a given analyte can provide indispensable support for site characterization, the development of numerical groundwater contamination models and remediation procedures when back diffusion occurs. In this study, within an industrial site in the province of Benevento (Italy), based on stratigraphy, a 3D hydrogeological model has been set up and coupled with results of natural gamma radioactivity logs to detect the release of Chromium VI from low-permeability lenses.

Keywords: HRSC; γ -ray; low permeability; contaminated site; characterization



Citation: Franchini, S.; De Filippi, F.M.; Barbieri, M.; Sappa, G. γ -Ray Log Tool for Detecting the Presence of Low-Permeability Lenses in High-Resolution Modelling of Contaminated Sites. *Water* **2023**, *15*, 3590. <https://doi.org/10.3390/w15203590>

Academic Editors: Marco Guida and Liliana Lefcariu

Received: 13 August 2023

Revised: 5 October 2023

Accepted: 9 October 2023

Published: 13 October 2023



Copyright: © 2023 by the authors. Licensee MDPI, Basel, Switzerland. This article is an open access article distributed under the terms and conditions of the Creative Commons Attribution (CC BY) license (<https://creativecommons.org/licenses/by/4.0/>).

1. Introduction

Water is regarded as one of the most important natural resources. Indeed, water resources and water quality are important and indispensable for human survival, the ecological environment, and sustainable economic and regional development [1,2].

In general, heavy metals, which are among the most common environmental pollutants, are released into the environment through natural processes or human activities such as industrial processes, leading to pollution with severe consequences [3]. Toxic metals in soils do not necessarily lead to toxicity because not all metal forms are toxic. Chromium (Cr) is one of the heavy metals considered dangerous to humans, and a slight increase in the level of Cr (VI) causes environmental and health problems due to its high toxicity, mutagenicity and carcinogenicity [4].

Rapid industrialization has led to an increase in the discharge of wastewater, including Cr (VI), and consequently to a rise in environmental pollution. Indeed, when metals are discharged, large proportions of metals settle in bottom sediments, while only small proportions of free metal ions remain dissolved in the water column [5,6].

In contaminated sites, the effectiveness of remediation measures is increasingly dependent on previous high-resolution site characterization (HRSC) results [7–11]. However, in many industrial sites with high pollution risk related to groundwater, hydrogeological

models are often based only on the stratigraphy results of geological drilling related to the groundwater monitoring network design. Even if suitable for modelling groundwater flow, this approach does not fit when contaminant back diffusion from low-permeability lenses and layers occurs at different points within high-permeability aquifers [12–15]. The contaminant release triggers might be the pumping time, changes in flow rates, or rapid raising or dropping of the water table, and the stakeholders often do not recognize them [16,17].

Throughout the hydrological cycle, more than 99% of pollutants are stored in sediments, which are aquatic systems' main sinks and carriers of contaminants [3,18].

Toxic metals of anthropic origin are mainly found as a labile extractable fraction in sediments. Indeed, they are generally introduced into the environment as hydrated ions or inorganic complexes and consequently can easily bind to the surface of sediment particles with relatively weak physical and chemical bonds [3,19].

A high-resolution local stratigraphy model can be obtained by coupling stratigraphic data with specific measurements in the monitoring wells, such as natural gamma radioactivity logs, multiparameter logs or other investigations for assessing soil hydraulic conductivity, as detailed as possible in the three-dimensional domain, involving not only the monitoring point but entire portions of the subsoil [20–22].

The natural gamma radioactivity measurements are performed along the depth of monitoring boreholes, detecting natural radioactivity emitted by geological formations according to their chemical mineralogical composition [23–26].

The most radioactive elements in sedimentary formations are the isotopes U238 and Th232 and the isotope K40 [20,25,26]. The concentrations of U and Th are similar in most sedimentary formations. In contrast, the concentration of K divides them into two groups: the clay minerals, with a relatively high concentration, and the rest, with an insignificant proportion. Therefore, these characteristics allow us to determine soil clay content by gamma ray log [20].

The log of natural gamma radioactivity is a measurement that can be performed along the depth inside boreholes of the natural radioactivity emitted by geological formations according to their chemical-mineralogical composition at a specific energy interval set by the recording system. Therefore, it is beneficial for lithostratigraphic reconstructions with the discrimination of clayey levels (impermeable) from sandy-gravel levels (permeable) [20].

In this way, it is possible to reconstruct the geological information inside existing wells for which there is insufficient stratigraphic information and to provide indispensable support for developing numerical models of the outflow and transport of water and contaminants. Natural radioactivity is a statistical phenomenon that does not present a constant value but strong oscillations concerning an average value, which characterizes its radioactivity.

This study aims to show how to improve a hydrogeological 3D model, coupling stratigraphic data and natural gamma radioactivity logs to detect the position and extension of low-permeability lenses and the release of Cr (VI) due to back diffusion phenomena. This has been successfully performed for the studied industrial site in Benevento (Campania Region—Italy), where high water table variations after seasonal rainfall patterns involve low-permeability lenses inducing higher pressure with the release of Cr (VI).

2. Geological and Hydrogeological Setting

The study site is located in the municipality of Benevento, under a large metallic components production plant.

The province of Benevento is located in the north-eastern sector of the Campania region in southern Italy and is known for its geological complexity [27].

The site is located in the northern part of the Campano-Lucano Apennines, more precisely in the Sannio area, between the south-eastern offshoots of the Monti del Matese (ridges of the Taburno and Camposauro mountains) and the south-western offshoots of the Monti Picentini (Mercogliano ridge—Monti di Avella).

The study area is located within an area dominated by river valleys through which the major rivers of the region flow. It is, therefore, an area rich in terrigenous deposits consisting mainly of clayey, sandstone and Plio-Pleistocene conglomerate successions. In particular, the outcropping deposits consist of coarse clastic and inhomogeneously lithified sequences [27,28].

The Calore Irpino is the province's main river and flows from south-east to west. In particular, the hydrographic network of the area in question is constituted by the Calore Irpino River in its middle course stretch and by the tributaries formed by the Tammaro on the right hydrographic side and the Sabato on the left. More precisely, the Tammaro River is about 150 m West of the site, while the Calore Irpino River is about 700 m away [27,29].

The Calore River, with a length of about 108 km and a mean annual flow discharge of $31.8 \text{ m}^3/\text{s}$, is the main tributary of the Volturno River, flowing into it in the hydrographic left. The Tammaro River is the primary right tributary of the Calore River, and it is about 68 km long with an average discharge of about $5 \text{ m}^3/\text{s}$. The morphology of the area where the site is inserted is purely hilly; in particular, the site is located at an altitude of approximately 140 m a.s.l. on the hydrographic left of the Tammaro River.

During the execution of the borings for the installation of the piezometers used to study the area, the following local stratigraphy was identified below the asphalt pavement up to the maximum depth investigated equal to 48 m b.g.l.:

- Clayey silt, with scattered dark brown clastic inclusions of centimetre dimensions up to a maximum depth of 6.2 m. This deposit is present in the western and south-eastern portion of the site with a thickness that tends to increase from north to south of the site;
- Sustained grain conglomerate, with pebbles of heterogeneous dimensions and in sandy, silty matrix, ochre-coloured matrix and half a meter thick, found at a depth of 2.5 m from ground level in the area south of the site;
- Silts, sometimes sandy with scattered clastic inclusions of dark brown-ochre colour at a depth from 4.2 to 6.2 m b.g.l. in the southern portion of the site;
- Poorly sorted deposit consisting of gravel, sand and silt, moderately thickened and sand-light brown. Clasts are generally polygenic and heteromorphic, with a modest degree of rounding. This deposit is found from ground level in the east, north-east portion of the site and in the west, south-west portion at a depth of 5–6 m from ground level, increasing the discovery depth from north to south of the site. This deposit is found in all the piezometers up to the maximum depth investigated (48 m b.g.l.). Between 24 and 31 m depths, a layer with the same characteristics but with a dark grey colour is present within this deposit.

The study was initially focused on the red dashed area, where spotted exceeding values of Chromium VI were found in groundwater samples. Based only on stratigraphic data, it was possible to build up the first local model, represented in Figure 1.

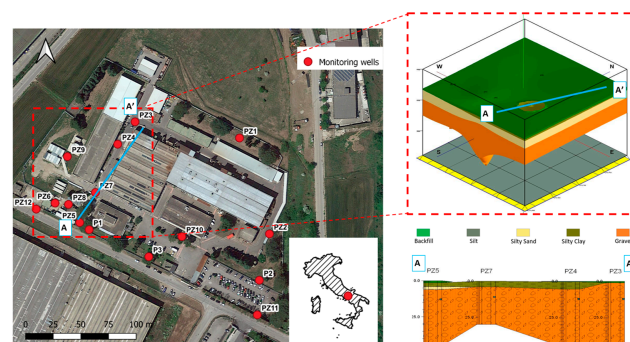


Figure 1. Monitoring network—within red dashed line, a focus on the area with major exceeding Cr (VI) values and the related geological model based only on stratigraphic data (right side). A geological cross section (A-A') is represented with the blue line.

3. Materials and Methods

In the study area, the environmental administrative procedure for remediation of the site was started in accordance with D.Lgs 152/06 art. 242, following the finding of exceeding the Contamination Threshold Concentrations (CSC) shown in Table 2, Annex 5, Part Four of D.Lgs 152/06 and s.m.i. (<https://www.gazzettaufficiale.it/dettaglio/codici/materiaAmbientale>, accessed on 4 October 2023) for the parameters total chromium and hexavalent chromium (Cr (VI)), relating to groundwater samples taken inside the water supply wells on site.

Following the notification, environmental investigations were carried out to verify the soil and groundwater environmental matrices' quality status within the site and in its vicinity, which involved the execution of 11 piezometers inside the site and 4 piezometers outside the site (Table 1). The monitoring wells were built to confirm the direction of the groundwater flow in the plant, the quality status of the groundwater in the critical areas, and any entry of contaminants from outside the site. Groundwater samples were taken for each piezometer for analysis (Table 2, Annex 5, Part Four of D.Lgs 152/06 and s.m.i., <https://www.gazzettaufficiale.it/dettaglio/codici/materiaAmbientale>, accessed on 4 October 2023) and piezometric measurements.

Table 1. Groundwater monitoring network data.

Piezometers	Depth (m b.g.l.)	Blind Section (m b.g.l.)	Well Screen (m b.g.l.)	Final Blind Section (m b.g.l.)
PZ 1	48	0–12	12–47	47–48
PZ 2	45	0–14	14–44	44–45
PZ 3	45	0–11	11–44	44–45
PZ 4	45	0–14.5	14.5–44	44–45
PZ 5	45	0–11	11–44	44–45
PZ 6	43	0–9	9–42	42–43
PZ 7	31	0–10	10–30	30–31
PZ 8	31	0–10	10–30	30–31
PZ 9	38	0–17	17–37	37–38
PZ 10	37	0–16	16–36	36–37
PZ 11	36	0–15	15–35	35–36
PZ 12	35	0–9	9–34	34–35
PZ 13	35	0–9	9–34	34–35
PZ 14	35	0–10	10–34	34–35
PZ 15	35	0–10	10–34	34–35

The 4 piezometers outside the site were built to check the quality of the groundwater to the west, downstream of the area, resulting in the highest concentrations of Cr (VI) within the site, to the east, downstream from the well, with excesses of Cr (VI) and in the western portion of the area south-east of the site. The piezometers were deepened with the bottom of the hole to guarantee a head of water of at least 20 m. In addition, the piezometric surveys and groundwater sampling were carried out for the execution of laboratory chemical analyses.

During the study, 3 piezometers were selected in which the greatest exceedances had been found for supplementary environmental investigations, which envisaged, for each piezometer (PZ6, PZ 7 and PZ8), the measurement of gamma radiation and the collection of groundwater samples at different depths. These investigations were carried out in static groundwater conditions.

The γ log readings were performed using the 2PGA-1000 probe, a scintillation probe equipped with a high-sensitivity NaI crystal and photomultiplier. In order to obtain high precision, the descent speed of the probe into the hole was kept lower than 3 m/min, adopting an adequate integration time.

Gamma-ray probes provide the result of the radioactivity at pre-established time intervals called integration time (1 s, 2 s, etc.), presenting the result after converting it in counts per second (cps) [25]. Then, after the data elaboration, with the help of Rockworks-22 software (released by Rockware Inc., serial number: RW20AST20930, Golden, CO, USA), a 3D-pixel geological model was reconstructed.

Furthermore, the data relating to the concentrations of Cr (VI) in the most polluted resulting piezometer (PZ8) were compared with the rainfall and hydrometric data taken from the website of the Civil Protection of the Campania Region (<http://centrofunzionale.regione.campania.it/#/pages/dashboard>, accessed on 4 October 2023). The data refer to the two measuring stations, “Paduli” and “Ponte Valentino”, located near the site studied.

4. Results

4.1. Environmental Investigations

The chemical analyses of the soil samples taken during the environmental investigations have shown total compliance with the regulatory limits set out in Table 1, Column B, Annex 5, Part Four of D.Lgs 152/06 and s.m.i. (<https://www.gazzettaufficiale.it/dettaglio/codici/materiaAmbientale>, accessed on 4 October 2023) for all the parameters searched.

Regarding the results of the chemical analyses carried out on the groundwater samples within the site, exceedances of CSC were detected for some potential inorganic contaminants, particularly total chromium and hexavalent chromium (Cr (VI)).

Comparing the maximum concentrations found at the time of contamination and the results obtained in the last monitoring campaign, Cr (VI) values decreased by one to two orders of magnitude in the wells inside the site called PZ5 (from 1000 µg/L to 210 µg/L) and PZ6 (100 µg/L to 3.02 µg/L). For PZ8, there was a significant increase in the concentrations of Cr (VI) measured, with a maximum measured value of 17,090 µg/L, followed by a gradual decrease with values in an order of magnitude of about 10 µg/L.

In the other piezometers on-site, the concentration of Cr (VI) always conforms with or is slightly higher than the threshold values in Table 2, Annex 5, Part Four of D.Lgs 152/06 and s.m.i. (<https://www.gazzettaufficiale.it/dettaglio/codici/materiaAmbientale>, accessed on 4 October 2023).

Regarding the presence of Cr (VI) outside the site’s boundaries, concentrations slightly higher than the reference CSC were detected only in the PZ12 piezometer. In the last monitoring campaign, in all piezometers, Cr (VI) values were recorded that complied with the CSC.

Considering that Cr (VI) has not been part of the plant’s production process for years, the temporary increase in Cr (VI) concentrations in PZ8 cannot be due to primary sources of contamination but to the activation of secondary sources. So, we compared the data of Cr (VI) concentrations recorded in PZ8 with the rainfall and hydrometric data of the monitoring stations closest to the study area. Since there are no substantial differences between the monitoring stations present in the area, only the data relating to the Ponte Valentino station are shown in Figure 2. With the aim of reducing the noise, a filter was applied to the rainfall and hydrometric data, using a moving average of 30 days.

It therefore appears that in December 2020–February 2021, there was an increase in rainfall corresponding to the rise in hydrometric levels from December 2020 to April 2021. In the same period, the Cr (VI) concentration recorded by PZ8 increased in January 2021, while in February 2021, it started to decrease again.

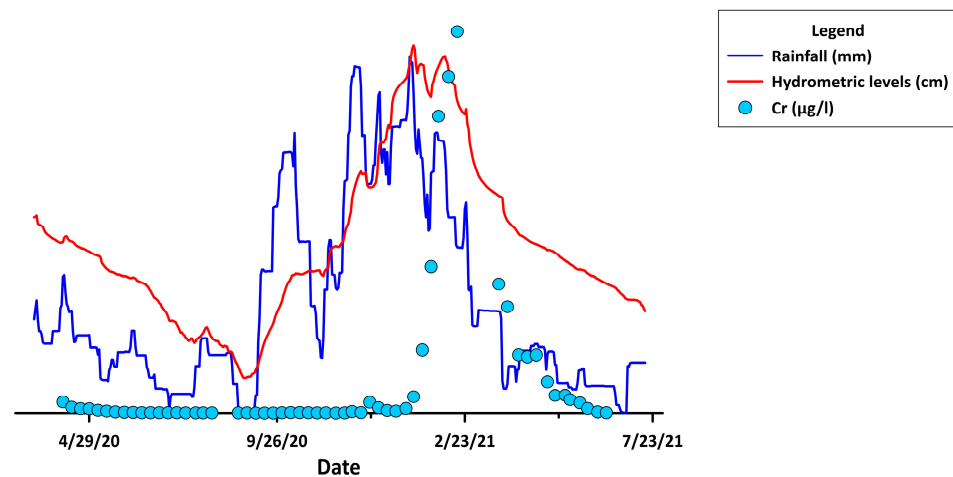


Figure 2. Time series from 1 March 2020 to 31 July 2021 showing comparison of Cr (VI) and hydrometric levels and rainfall recorded in Ponte Valentino Station.

4.2. γ -Ray Investigations

The radioactivity γ core drilling was carried out at different depths in the three selected piezometers: in PZ6 up to a depth of 41 m, in PZ7 up to a depth of 30.5 m and in PZ8 up to a depth of 29.5 m. The corresponding profiles were recorded during descent and ascent, but in the graphic elaboration, the average of both profiles is reported (Figure 3).

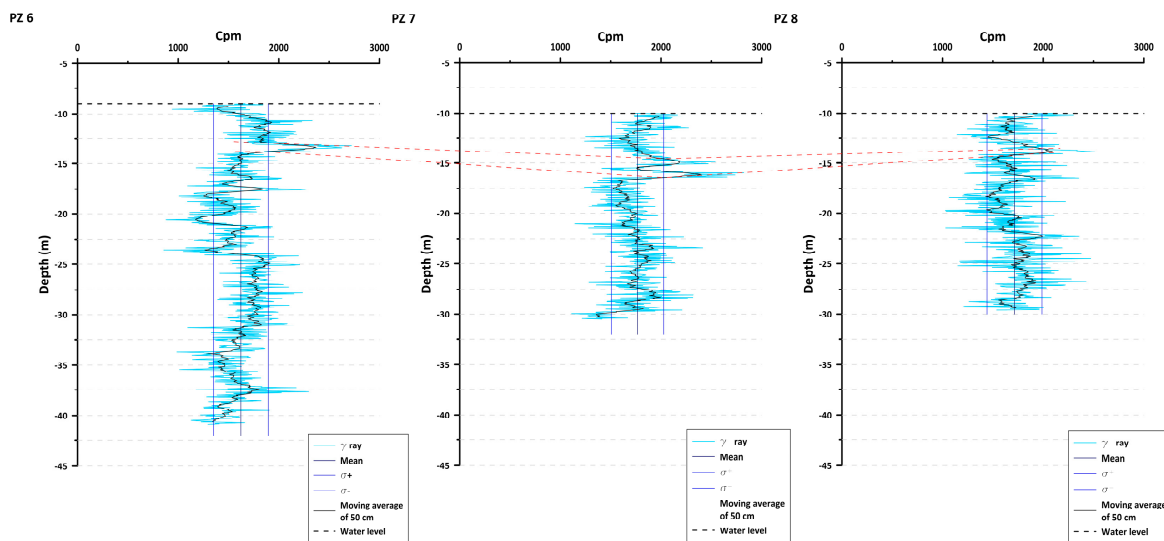


Figure 3. Gamma log data processing in PZ6, PZ7 and PZ8 for the detection of low-permeability layers. The dotted red line indicates the identified clay lens.

With the aim of reducing the noise, a filter was applied to the time series, using a moving average of 50 cm. In addition, the values recorded in the blind section of the piezometer were excluded, as the registered data referred to the borehole case and not to the soil, and only the data recorded in the cracked section were considered. A statistical data evaluation led to the calculation of $\sigma+$ and $\sigma-$, which are given by the sum of the mean and the standard deviation and the difference between the mean and the standard deviation, respectively. The peaks highlighted beyond the $\sigma+$ value represent the levels with higher concentrations of radioactive elements and, therefore, indicate the presence of levels or lenses with a higher clayey concentration (impermeable). Meanwhile, the peaks that are highlighted below the $\sigma-$ value represent the levels or lenses with lower concentrations of radioactive elements and, therefore, indicate the presence of more sandy-gravel levels (permeable).

In detail, a positive peak was recorded for all three piezometers, indicating a clay level (impermeable) between 13 and 15 m deep. In the case of the PZ7, there was a positive peak even at 16 m depth. The negative peaks, therefore indicated the sandy-gravel levels (permeable) were recorded in PZ6 between 20 and 21 m deep and 24 m deep, and in PZ7 up to 30 m deep (Figure 3).

5. Discussion

The graph in Figure 2 shows how the concentrations of Cr (VI) in the PZ8 follow the trend of rains and hydrometric levels. More in detail, it is possible to observe how the concentration trend of Cr (VI) decreases suddenly, just like the rains. The fact that Cr (VI) follows the rainfall trend and not the hydrometric levels indicates that this is a local pollution phenomenon. It is, therefore, not a source of pollution transported from very far away with the rivers present in the area, but it can be assumed that there is a hypothetical source of pollution not far from the site.

Based on the results from γ -ray investigations, a new and more detailed 3D geological model of the study area has been set up coupling available stratigraphy and natural γ radioactivity logs elaboration (Figures 4 and 5). The aim was to detect the release of Cr (VI) from low-permeability lenses at specific depths. This study demonstrated the useful tool of γ log investigations for lithostratigraphic reconstruction, with the discrimination of thin clayey levels or lenses, responsible for the slow release of contaminants within a sandy-gravel thick aquifer.

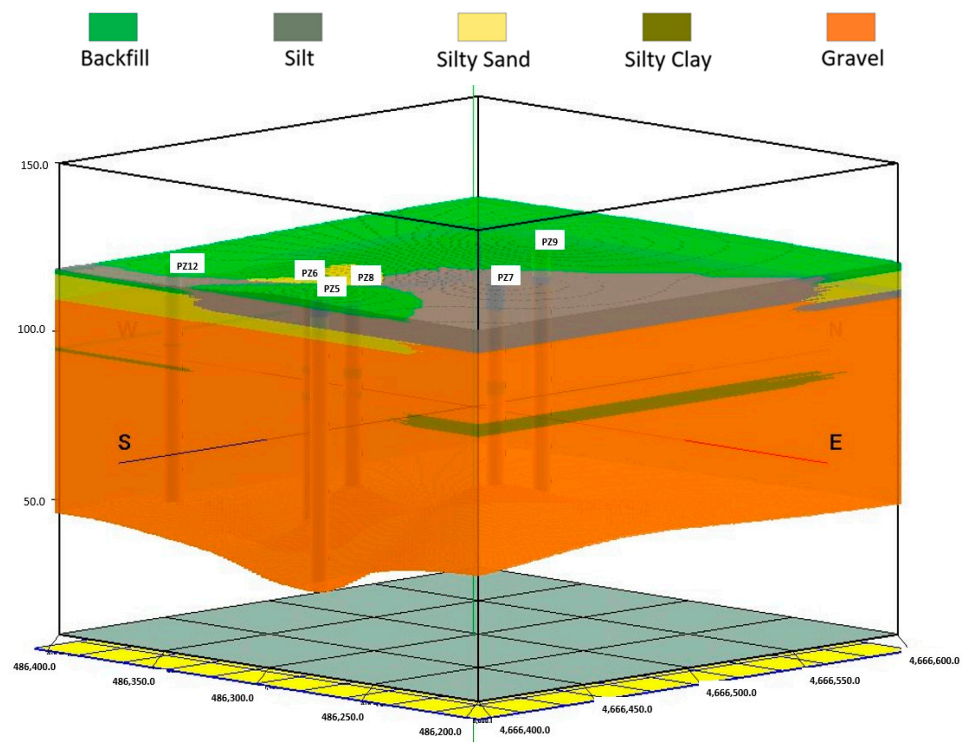


Figure 4. Enhanced 3D pixel geological model of the study area based on γ -ray log results.

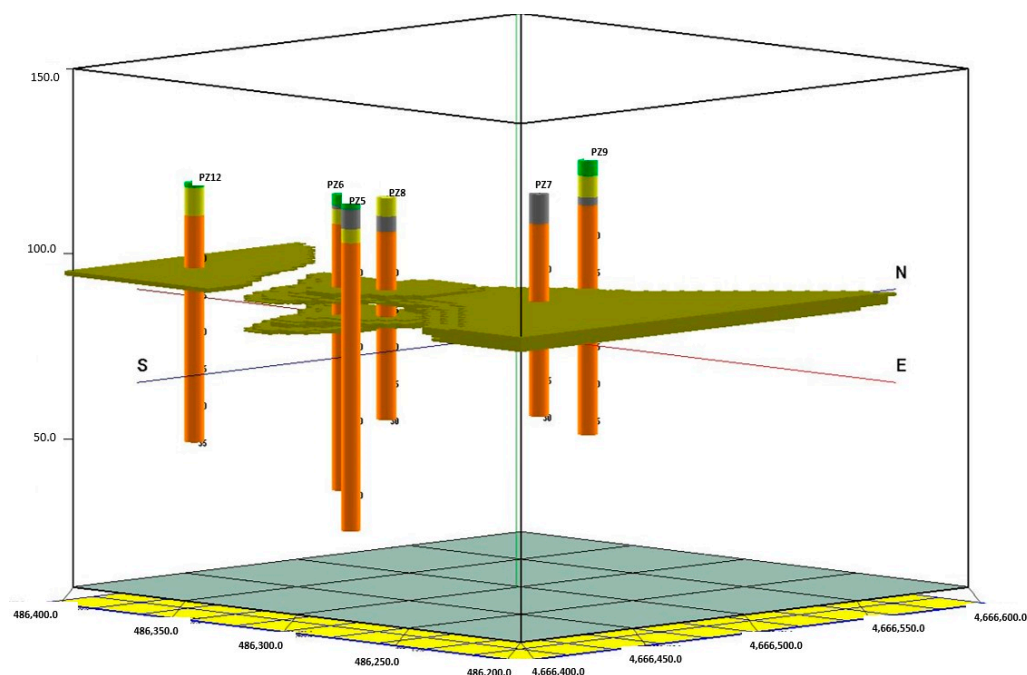


Figure 5. Detail of the 3D extension of low-permeability layers modelled.

As we can see in Figure 3, in the study area, there is a stratification with a different permeability, with more permeable levels consisting of sandy-gravelly deposits and less permeable levels consisting of clay lenses. Water passes and filters the most permeable horizons more quickly, but during the increase in hydraulic load due to the increase in rainfall, water also involves the less permeable horizons.

Furthermore, to confirm these results, stratigraphic logs produced during the execution of the piezometers and the granulometric analyses were also analysed. In particular, for PZ8, the stratigraphic log is constituted by calcareous breccia with angular clasts with a poor silty-sandy matrix, with an increase in the sandy fraction with depth, alternating with more silty-sandy levels.

Moreover, the soil sample taken in the saturated zone has a composition made up of 61% sand, 22% silt and 17% clay. So, these data attest that there is a significant percentage of clay.

In these soils consisting of limestone breccias, it is sufficient to have a presence of clay, which saturates the interstitial voids in the breccia to ensure that permeability is significantly reduced.

Since the PZ 8 has always been pumped, it has drawn towards itself the polluted water, meaning that the clay levels identified have captured the pollutant.

The increase in the piezometric level and, therefore, the variation in the interstitial pressure have favoured the release of Cr (VI) that has settled in a clay lens and that, once put in motion, follows a preferential way that goes through the PZ8. It also slightly affects PZ7, while it does not get to PZ6 downstream of PZ8.

This explains why, in areas where contamination seems to be resolved, suddenly, there is a high pollution concentration, even though it is no longer present in the production processes of the plants. Indeed, pollutants tend to accumulate in sediment; in particular, the adsorption capacity increases with the decrease in particle size.

The new 3D model is built based on the processing of gamma-log results, thus identifying clayey levels within the limestone breccia. The new model is a pixel lithological model (more detailed than the simple stratigraphic model with homogeneous bands). The nearest neighbour geostatistical method was used to reconstruct the model (Figure 4).

In Figure 5, the single clay formation is represented as isolated in the domain of the other geological layers.

6. Conclusions

In conclusion, in areas affected by pollution, years of heavier rains induce a rise in the piezometric level that involves the movement of pollutants nestled in less permeable horizons that are engaged during a higher hydraulic head. Therefore, it is not a new contamination phenomenon but simply a release of contaminants still present in the area.

In this context, the use of gamma rays in combination with the analysis of the pluviometric and hydrometric data, and together with the time series of the concentrations of a given analyte, help to understand the phenomena that induce the subsequent releases of pollutants despite the following of all safety measures in the area subject to pollution. In particular, the tool of gamma ray log investigations is proven to be very useful for lithostratigraphic reconstruction, with the discrimination of thin clayey levels or lenses within a sandy-gravel thick aquifer in alluvial heterogeneous context responsible for the slow release of contaminants in time [30,31].

In sites with a high risk of groundwater pollution, the use of these tools, together with further investigations, such as the measurement of the concentration of the pollutant absorbed by levels with different permeability (through the use of XRF), can provide a reasonable basis for identifying the most vulnerable areas. This makes it possible to reduce remediation costs and times as it is possible to identify the areas in which it is necessary to deepen groundwater management.

Author Contributions: Conceptualization, G.S. and M.B.; methodology, F.M.D.F. and S.F.; software, F.M.D.F.; validation G.S. and M.B.; investigation, F.M.D.F.; data curation, S.F.; writing—original draft preparation, F.M.D.F. and S.F.; writing—review and editing, G.S. and M.B.; supervision, G.S. and M.B.; project administration, G.S.; funding acquisition, G.S. All authors have read and agreed to the published version of the manuscript.

Funding: This research received no external funding.

Data Availability Statement: Not applicable.

Conflicts of Interest: The authors declare no conflict of interest.

References

1. Xiao, J.; Wang, L.; Deng, L.; Jin, Z. Characteristics, Sources, Water Quality and Health Risk Assessment of Trace Elements in River Water and Well Water in the Chinese Loess Plateau. *Sci. Total Environ.* **2019**, *650*, 2004–2012. [[CrossRef](#)] [[PubMed](#)]
2. Long, J.; Luo, K. Elements in Surface and Well Water from the Central North China Plain: Enrichment Patterns, Origins, and Health Risk Assessment. *Environ. Pollut.* **2020**, *258*, 113725. [[CrossRef](#)] [[PubMed](#)]
3. Bartoli, G.; Papa, S.; Sagnella, E.; Fioretto, A. Heavy Metal Content in Sediments along the Calore River: Relationships with Physical-Chemical Characteristics. *J. Environ. Manag.* **2012**, *95*, S9–S14. [[CrossRef](#)] [[PubMed](#)]
4. Al-Battashi, H.; Joshi, S.J.; Pracejus, B.; Al-Ansari, A. The Geomicrobiology of Chromium (VI) Pollution: Microbial Diversity and Its Bioremediation Potential. *Open Biotechnol. J.* **2016**, *10*, 379–389. [[CrossRef](#)]
5. Gaur, V.K.; Gupta, S.K.; Pandey, S.D.; Gopal, K.; Misra, V. Distribution of Heavy Metals in Sediment and Water of River Gomti. *Environ. Monit. Assess.* **2005**, *102*, 419–433. [[CrossRef](#)] [[PubMed](#)]
6. Aradpour, S.; Noori, R.; Tang, Q.; Bhattarai, R.; Hooshyaripor, F.; Hosseinzadeh, M.; Haghghi, A.T.; Klöve, B. Metal Contamination Assessment in Water Column and Surface Sediments of a Warm Monomictic Man-Made Lake: Sabalan Dam Reservoir, Iran. *Hydrol. Res.* **2020**, *51*, 799–814. [[CrossRef](#)]
7. Dijkshoorn, P.; Mori, P.; Zaffaroni, M.C. High Resolution Site Characterization as Key Element for Proper Design and Cost Estimation of Groundwater Remediation. *Acque Sotter.-Ital. J. Groundw.* **2014**, *3*, 17–27. [[CrossRef](#)]
8. Streeter, M.T.; Vogelgesang, J.; Schilling, K.E.; Burras, C.L. Use of High-Resolution Ground Conductivity Measurements for Denitrifying Conservation Practice Placement. *Environ. Monit. Assess.* **2022**, *194*, 784. [[CrossRef](#)]
9. Liu, G.; Butler, J.J.; Bohling, G.C.; Reboulet, E.; Knobbe, S.; Hyndman, D.W. A New Method for High-Resolution Characterization of Hydraulic Conductivity. *Water Resour. Res.* **2009**, *45*, 8. [[CrossRef](#)]
10. Liu, G.; Butler, J.J.; Reboulet, E.; Knobbe, S. Bestimmung von Vertikalprofilen Der Hydraulischen Durchlässigkeit Mit Direct Push-Methoden. *Grundwasser* **2012**, *17*, 19–29. [[CrossRef](#)]
11. Vienken, T.; Kreck, M.; Hausmann, J.; Werban, U.; Dietrich, P. Innovative Strategies for High Resolution Site Characterization: Application to a Flood Plain. *Acque Sotter.-Ital. J. Groundw.* **2014**, *3*, 7–14. [[CrossRef](#)]
12. You, X.; Liu, S.; Dai, C.; Guo, Y.; Zhong, G.; Duan, Y. Contaminant Occurrence and Migration between High- and Low-Permeability Zones in Groundwater Systems: A Review. *Sci. Total Environ.* **2020**, *743*, 140703. [[CrossRef](#)] [[PubMed](#)]

13. Bolhari, A.; Sale, T. Processes Governing Treatment of Contaminants in Low Permeability Zones. *Sci. Total Environ.* **2023**, *879*, 163010. [[CrossRef](#)] [[PubMed](#)]
14. Borden, R.C.; Cha, K.Y. Evaluating the Impact of Back Diffusion on Groundwater Cleanup Time. *J. Contam. Hydrol.* **2021**, *243*, 103889. [[CrossRef](#)]
15. Yang, M.; Annable, M.D.; Jawitz, J.W. Back Diffusion from Thin Low Permeability Zones. *Environ. Sci. Technol.* **2015**, *49*, 415–422. [[CrossRef](#)]
16. Brooks, M.C.; Yarney, E.; Huang, J. Strategies for Managing Risk Due to Back Diffusion. *Groundw. Monit. Remediat.* **2021**, *41*, 76–98. [[CrossRef](#)]
17. Blue, J.; Boving, T.; Tuccillo, M.E.; Koplos, J.; Rose, J.; Brooks, M.; Burden, D. Contaminant Back Diffusion from Low-Conductivity Matrices: Case Studies of Remedial Strategies. *Water* **2023**, *15*, 570. [[CrossRef](#)]
18. Filgueiras, A.V.; Lavilla, I.; Bendicho, C. Evaluation of Distribution, Mobility and Binding Behaviour of Heavy Metals in Surficial Sediments of Louro River (Galicia, Spain) Using Chemometric Analysis: A Case Study. *Sci. Total Environ.* **2004**, *330*, 115–129. [[CrossRef](#)]
19. Jain, C.K.; Gupta, H.; Chakrapani, G.J. Enrichment and Fractionation of Heavy Metals in Bed Sediments of River Narmada, India. *Environ. Monit. Assess.* **2008**, *141*, 35–47. [[CrossRef](#)]
20. De Filippi, F.M.; Sappa, G. Combined Well Multi-Parameter Logs and Low-Flow Purging Data for Soil Permeability Assessment and Related Effects on Groundwater Sampling. *Hydrology* **2023**, *10*, 12. [[CrossRef](#)]
21. Vitale, S.A.; Robbins, G.A. Characterizing Groundwater Flow in Monitoring Wells by Altering Dissolved Oxygen. *Groundw. Monit. Remediat.* **2016**, *36*, 59–67. [[CrossRef](#)]
22. Knight, R.; Walsh, D.O.; Butler, J.J.; Grunewald, E.; Liu, G.; Parsekian, A.D.; Reboulet, E.C.; Knobbe, S.; Barrows, M. NMR Logging to Estimate Hydraulic Conductivity in Unconsolidated Aquifers. *Groundwater* **2016**, *54*, 104–114. [[CrossRef](#)] [[PubMed](#)]
23. Kluso, J. Environmental Monitoring and in Situ Gamma Spectrometry. *Radiat. Phys. Chem.* **2001**, *61*, 209–216. [[CrossRef](#)]
24. Ciupek, K.; Jednoróg, S.; Fujak, M.; Szewczak, K. Evaluation of Efficiency for in Situ Gamma Spectrometer Based upon Cerium-Doped Lanthanum Bromide Detector Dedicated for Environmental Radiation Monitoring. *J. Radioanal. Nucl. Chem.* **2014**, *299*, 1345–1350. [[CrossRef](#)]
25. Díaz-Curiel, J.; Miguel, M.J.; Biosca, B.; Arévalo-Lomas, L. Gamma Ray Log to Estimate Clay Content in the Layers of Water Boreholes. *J. Appl. Geophys.* **2021**, *195*, 104481. [[CrossRef](#)]
26. Moshupya, P.M.; Mohuba, S.C.; Abiye, T.A.; Korir, I.; Nhleko, S.; Mkhosi, M. In Situ Determination of Radioactivity Levels and Radiological Doses in and around the Gold Mine Tailing Dams, Gauteng Province, South Africa. *Minerals* **2022**, *12*, 1295. [[CrossRef](#)]
27. Revellino, P.; Guerriero, L.; Mascellaro, N.; Fiorillo, F.; Grelle, G.; Ruzza, G.; Guadagno, F.M. Multiple Effects of Intense Meteorological Events in the Benevento Province, Southern Italy. *Water* **2019**, *11*, 1560. [[CrossRef](#)]
28. Revellino, P.; Grelle, G.; Donnarumma, A.; Guadagno, F.M. Structurally Controlled Earth Flows of the Benevento Province (Southern Italy). *Bull. Eng. Geol. Environ.* **2010**, *69*, 487–500. [[CrossRef](#)]
29. Magliulo, P. Quaternary Deposits and Geomorphological Evolution of the Telesina Valley (Southern Apennines). *Geogr. Fis. Din. Quat.* **2005**, *28*, 125–146.
30. Ding, X.H.; Feng, S.J.; Zheng, Q.T. Forward and Back Diffusion of Reactive Contaminants through Multi-Layer Low Permeability Sediments. *Water Res.* **2022**, *222*, 118925. [[CrossRef](#)]
31. De Filippi, F.M.; Iacurto, S.; Ferranti, F.; Sappa, G. Hydraulic Conductivity Estimation Using Low-Flow Purging Data Elaboration in Contaminated Sites. *Water* **2020**, *12*, 898. [[CrossRef](#)]

Disclaimer/Publisher’s Note: The statements, opinions and data contained in all publications are solely those of the individual author(s) and contributor(s) and not of MDPI and/or the editor(s). MDPI and/or the editor(s) disclaim responsibility for any injury to people or property resulting from any ideas, methods, instructions or products referred to in the content.